

Modified affine arithmetic based continuation power flow analysis for voltage stability assessment under uncertainty

ISSN 1751-8687
 Received on 8th May 2018
 Revised 30th June 2018
 Accepted on 25th July 2018
 E-First on 7th September 2018
 doi: 10.1049/iet-gtd.2018.5479
 www.ietdl.org

Bala Surendra Adusumilli¹ ✉, Boddeti Kalyan Kumar¹

¹Department of Electrical Engineering, Indian Institute of Technology Madras, Chennai, India

✉ E-mail: abs219@gmail.com

Abstract: Continuation power flow (CPF) analysis has been used in the literature to determine the voltage collapse point from active power versus voltage curves (PV curves) for steady-state voltage stability assessment. Affine arithmetic-based (AA) CPF analysis to determine PV curve bounds under uncertainty in power generation was introduced in the literature to overcome the problem of large computational time with Monte Carlo (MC) simulations, by getting a faster solution with a reasonably good accuracy. However, AA operations lead to more noise terms and hence overestimation of bounds. In the present work, a modified AA (modAA)-based CPF analysis is proposed to determine PV curve bounds by considering uncertainties associated with active and reactive power injections at all buses in the system. The proposed method reduces the overestimation caused by the AA operations and gives more accurate solution bounds. The proposed modAA-based CPF analysis is tested on 5-bus test case, IEEE 57, European 1354 and Polish 2383-bus systems. The simulation results with the proposed method are compared with MC simulations and AA-based CPF analysis to show the efficacy of the proposed method.

1 Introduction

Long-term voltage stability can be assessed with the use of static/steady-state analysis techniques [1]. Continuation power flow (CPF) analysis is one of the most frequently used tools for static voltage stability analysis which is used to draw power versus voltage curves (PV curves) at any bus in the system. From PV curves, maximum loadability/steady-state voltage stability limit/critical point can be determined. If the system is loaded beyond the critical point, the voltage will collapse. This is an important information for power system operator for reliable operation of power systems [1]. CPF using predictor–corrector method with local parameterisation was first proposed in [2]. Later, a computer package for CPF was introduced in [3]. To overcome the difficulties of Jacobian singularity, geometric parameterisation-based CPF was proposed in [4, 5]. Recently, numerical polynomial homotopy continuation method was introduced in [6] without the need of handling bifurcations to find all solutions. However, the methods proposed in [2–6] are for a deterministic set of loads and generations. These methods cannot give an accurate estimation of maximum loadability when uncertainties are associated with loads and generator powers. The sources of uncertainty could be due to measurement errors, forecasting errors, intermittent power generation sources such as wind and solar, round-off, truncation errors etc. Probabilistic-based methods were first used in order to include uncertainty into voltage stability analysis, where each uncertain variable is assumed to have a certain probability distribution function and a large number of samples are collected to get various loading and generation scenarios. Conventional analysis techniques can be used for solving each of these large numbers of samples. This method is called Monte Carlo (MC) simulations. MC simulations based voltage stability analysis was given in [7, 8]. However, MC simulations take more time and are computationally burdensome [9]. A two-point estimate method was used in [9] as an alternative to MC simulations but it is not as accurate as MC simulations. A higher-order point estimate is required to achieve higher accuracy but it increases the computational burden. In [10], a truncated Taylor series expansion was used to determine reliability margins but it assumes that the uncertainties are independent. A faster way of computing voltage stability indices by a sensitivity analysis that uses linearisation techniques was proposed in [11, 12] but linearisation is valid only

under certain conditions. In [13], uncertainty representation using fuzzy set theory has been proposed. In methods [7–13], there is a trade-off between accuracy and computational time. More accurate methods take more computational time and on the other hand methods with less computational time do not give accurate results or the inter-dependencies between the uncertain variables are not considered. There is always a compromise between accuracy and computational cost. A self-validated range arithmetic method called affine arithmetic (AA) can be used for uncertainty analysis that requires less computational cost and gives reasonably good accuracy, also inter-dependencies among all uncertain variables are taken into account. In [14], AA-based power flow analysis was first proposed that considered uncertainties associated with active and reactive power injections. In [15], optimal power flow using AA was proposed.

For voltage stability studies, an AA-based CPF to compute PV curve bounds that considers the uncertainty in intermittent sources of power generation was first proposed in [16] to achieve good accuracy with less computational cost. AA multiplication in [16] has the disadvantages of extra noise term generation and the quadratic relation between noises is neglected which causes an overestimation of solution bounds. In [17], a modified AA (modAA) multiplication is proposed, which distributes the additional noise term among the existing noise terms proportionally and can reduce the overestimation as in [16], and can lead to tighter solution bounds. In the present work, the modAA proposed in [17] is used to solve CPF with uncertainty in both loads and generation. The proposed modified affine multiplication-based CPF can reduce this overestimation and tighter solution bounds can be achieved. The proposed method is implemented on 5-bus test case, IEEE 57, European 1354 and Polish 2383-bus systems and results are compared with AA-based CPF [16] and MC-based CPF [7].

The rest of this paper is organised as follows: Section 2 describes the CPF analysis for the deterministic set of loads and generation. Section 3 gives the brief description of AA operations followed by CPF analysis using AA. Section 4 describes the modAA multiplication and its application to AA-based CPF analysis. Section 5 presents the detailed simulation results. The conclusions are given in Section 6.

2 CPF analysis

CPF analysis is a method of finding the power flow solution at each loading condition when the load is increased step-by-step from the base case. Bus voltage reaches a critical point or steady-state voltage stability limit with an increase in load, beyond which the voltage will collapse. CPF uses predictor–corrector method of finding the next solution on the curve from the starting point, i.e. from the base load point. PV curves at any bus in the system can be obtained from the output of CPF.

The active power and reactive power balance equations, at each bus in a system are reformulated in order to include the loading factor (λ) as follows:

$$P_{g,i,0}(1 + \lambda K_{g_i}) - P_{l,i,0}(1 + \lambda K_{l_i}) = P_i, \quad i = 1, 2, \dots, N_P \quad (1)$$

$$Q_{g,i,0} - Q_{l,i,0}(1 + \lambda K_{l_i}) = Q_i, \quad i = 1, 2, \dots, N_Q \quad (2)$$

$$Q_{l,i,0} = P_{l,i,0} \times \tan(\Psi_i), \quad i = 1, 2, \dots, N_Q \quad (3)$$

where

$$P_i = \sum_{k=1}^N |V_i| |V_k| [G_{ik} \cos(\delta_i - \delta_k) + B_{ij} \sin(\delta_i - \delta_k)] \quad (4)$$

$$Q_i = \sum_{k=1}^N |V_i| |V_k| [G_{ik} \sin(\delta_i - \delta_k) - B_{ij} \cos(\delta_i - \delta_k)] \quad (5)$$

where $P_{g,i,0}$, $Q_{g,i,0}$ are specified or base-case active and reactive power generations at the i th bus, respectively. $P_{l,i,0}$, $Q_{l,i,0}$ are specified or base-case active and reactive powers drawn by loads at the i th bus, respectively. $|V_i|$, $|V_k|$ are bus voltage magnitudes at buses i and k , respectively. G_{ik} , B_{ik} are conductance and susceptance of (i, k) th element in the Y -bus matrix. δ_i , δ_k are bus voltage angles at buses i and k , respectively. N is total number of buses in the system. N_P is total number of buses at which P is specified (excluding slack bus). N_Q is total number of buses at which Q is specified. λ is the loading factor such that $(0 \leq \lambda \leq \lambda_{cr})$. $\lambda = 0$ corresponds to base load and $\lambda = \lambda_{cr}$ corresponds to the critical load (i.e. steady-state voltage stability limit). K_{l_i} , K_{g_i} are constants used to specify the rate of change in load power and generator power at the i th bus, respectively, as λ varies. Ψ_i is the load power factor angle at the i th bus.

The non-linear algebraic equations (1)–(5) can be represented as

$$f(\delta, V, \lambda) = 0 \quad (6)$$

In deterministic CPF, (1)–(5) are solved at different loading conditions by using a well-established curve tracing approach, ‘Predictor–Corrector method’. Starting from an initial known solution corresponding to base case ($\lambda = 0$), this method traces the full PV curve. In the predictor step, an approximate solution can be obtained by calculating the tangent vector from the initial solution point. The local parameterisation technique with the voltage at a load bus taken as continuation parameter has the advantage of not needing to switch between continuation parameters [16] to trace the full PV curve.

In the corrector step, the predicted solution is taken as the initial values and the conventional Newton–Raphson method is used to solve the equations given in (7). The actual set of non-linear power balance equations is augmented by one equation corresponding to the local parameterisation

$$\begin{bmatrix} f(\delta, V, \lambda) \\ V_k - V_k^p \end{bmatrix} = 0 \quad (7)$$

where V_k^p is the predicted value of the k th bus voltage. Here, k corresponds to the bus which has the largest rate of change of

voltage magnitude with respect to load changes. Starting from the k th load bus voltage corresponding to base load, the voltage is decreased step-by-step and the corresponding λ is determined by the predictor–corrector approach. From now onwards, the CPF for deterministic loads and generation is termed as det-CPF.

3 AA-based CPF

The det-CPF described so far in Section 2 gives PV curve bounds for deterministic input, i.e. for a particular set of power generations and demands. Whenever the power injections at the buses represent an uncertainty range, the state variables and outputs in the system also represent a range of values. So, a range arithmetic technique called AA was proposed in [18], for solving CPF with uncertainty, labelled as AA-CPF, is described below.

3.1 Affine arithmetic

In AA, each uncertain variable is represented by an affine form, i.e. first degree polynomial comprises of its central value and partial deviations which shows the correlation among various variables as follows:

$$\hat{u} = u_0 + u_1 \epsilon_1 + u_2 \epsilon_2 + \dots + u_n \epsilon_n \quad (8)$$

where u_0 is the central value of the affine form. u_1, u_2, \dots, u_n are the partial deviations representing the magnitudes of the corresponding uncertainty. $\epsilon_1, \epsilon_2, \dots, \epsilon_n$ are the noises that represent independent sources of uncertainties and they lie within $[-1, +1]$.

In AA, mathematical operations on uncertain variables are broadly classified into (i) affine operations and (ii) non-affine operations. The result of affine operations is strictly an affine form. Basic affine operations on generalised variables \hat{u} , \hat{v} are given as follows:

$$\begin{aligned} \hat{u} + \hat{v} &= (u_0 \pm v_0) + (u_1 \pm v_1) \epsilon_1 + \dots + (u_n \pm v_n) \epsilon_n \\ a\hat{u} &= (au_0) + (au_1) \epsilon_1 + (au_2) \epsilon_2 + \dots + (au_n) \epsilon_n \\ \hat{u} \pm b &= (u_0 \pm b) + u_1 \epsilon_1 + u_2 \epsilon_2 + \dots + u_n \epsilon_n \end{aligned} \quad (9)$$

where $a, b \in R$.

Any mathematical operation other than (9) is a non-affine operation, the result of which is a non-affine form and is approximated to affine form using Chebyshev approximations [18]. Multiplication of two affine forms is the most frequently used non-affine operation. Suppose $\hat{u} = (u_0 + \sum_{i=1}^n u_i \epsilon_i)$ and $\hat{v} = (v_0 + \sum_{i=1}^n v_i \epsilon_i)$, then their multiplication can be given by

$$\hat{u} \times \hat{v} = u_0 v_0 + \sum_{i=1}^n (v_0 u_i + u_0 v_i) \epsilon_i + \left(\sum_{i=1}^n u_i \epsilon_i \right) \left(\sum_{i=1}^n v_i \epsilon_i \right) \quad (10)$$

The last term in (10) is approximated by the radius operator for an affine variable denoted by $R(\hat{u})$ which is the radius of the AA variable \hat{u} and it is given as $R(\hat{u}) = \sum_{i=1}^n |u_i|$.

Hence, (10) can be approximated as follows:

$$\hat{u} \times \hat{v} = u_0 v_0 + \sum_{i=1}^n (v_0 u_i + u_0 v_i) \epsilon_i + R(\hat{u}) R(\hat{v}) \Lambda \quad (11)$$

where Λ is a new noise term introduced due to the non-affine operation and is also given by the interval $[-1, 1]$.

3.2 PV curve computation using AA-CPF

In AA-CPF, the curve tracing procedure uses a predictor–corrector method along with local parameterisation and is same as in det-CPF that is described in Section 2. As the active and reactive power injections are a range of values, the state variables of the system also represent a range. The bus voltage magnitude and angle in affine form are represented as follows:

$$\widehat{V}_i = V_i^0 + \sum_{j=1}^{N_P} V_{ij}^P \epsilon_{P_j} + \sum_{k=1}^{N_Q} V_{ik}^Q \epsilon_{Q_k} \quad \text{for } i = 1, 2, \dots, N_Q \quad (12)$$

$$\widehat{\delta}_i = \delta_i^0 + \sum_{j=1}^{N_P} \delta_{ij}^P \epsilon_{P_j} + \sum_{k=1}^{N_Q} \delta_{ik}^Q \epsilon_{Q_k} \quad \text{for } i = 1, 2, \dots, N_P \quad (13)$$

$$\widehat{\lambda} = \lambda^0 + \sum_{j=1}^{N_P} \lambda_j^P \epsilon_{P_j} + \sum_{k=1}^{N_Q} \lambda_k^Q \epsilon_{Q_k} \quad (14)$$

where \widehat{V}_i , $\widehat{\delta}_i$ are voltage magnitude and angle, respectively, at the i th bus in affine form. $\widehat{\lambda}$ is the loading factor λ in affine form. V_i^0 , δ_i^0 are the central values of the i th bus voltage magnitude and angle, respectively. λ^0 is the central value of loading parameter λ which is obtained from det-CPF. V_{ij}^P , δ_{ij}^P are partial deviations of the i th bus voltage magnitude and angle due to active power injected at the j th bus, respectively. V_{ik}^Q , δ_{ik}^Q are partial deviations of the i th bus voltage magnitude and angle due to reactive power injected at the k th bus, respectively. λ_j^P , λ_k^Q are partial deviations of λ due to active and reactive powers injected at the j th and k th buses, respectively. ϵ_{P_j} , ϵ_{Q_k} are noise intervals representing the uncertainty of active and reactive power injections at the j th and k th buses, respectively.

The central values: V_i^0 , δ_i^0 and λ^0 and partial deviations: V_{ij}^P , V_{ik}^Q , δ_{ij}^P , δ_{ik}^Q and λ_j^P , λ_k^Q are obtained by solving (1)–(5) from det-CPF as given in Section 2.

The affine forms of voltage magnitude, angle and loading factor given in (12)–(14) are substituted in power balance equations (1)–(5) and they contain sine and cosine non-linear operations. Sine and cosine of AA variables are expanded using Chebyshev polynomial of first kind using recurrence relation given in [19].

The power balance equations (1) and (2) are now in affine form and are given as follows:

$$\widehat{P}_{g_i}(1 + \widehat{\lambda}K_{g_i}) - \widehat{P}_{l_i}(1 + \widehat{\lambda}K_{l_i}) = \widehat{P}_i, \quad i = 1, 2, \dots, N_P \quad (15)$$

$$Q_{g_i} - \widehat{Q}_{l_i}(1 + \widehat{\lambda}K_{l_i}) = \widehat{Q}_i, \quad i = 1, 2, \dots, N_Q \quad (16)$$

where $\widehat{P}_{g_i} = [P_{g_i}^{\min} P_{g_i}^{\max}]$ and $\widehat{P}_{l_i} = [P_{l_i}^{\min} P_{l_i}^{\max}]$ are the specified power intervals of generators and loads. The interval range depends on the percentage of uncertainty included in the analysis. The equation corresponding to the local parameterisation is given in (17)

$$\widehat{V}_{\text{load}} = V_k \quad (17)$$

Equations (15)–(17) in affine form are solved to obtain PV curve bounds. V_k in (17) is the k th bus voltage which experiences the largest rate of change of voltage with respect to load change. The voltage V_k is updated in each step in order to trace the full PV curve as given below:

$$V_k = V_k - \Delta V_k \quad (18)$$

where ΔV_k is the step size and its value depends on at which portion of the PV curve is being traced. Smaller step sizes are required near or at the maximum loadability point. Maximum loadability point can be identified when the loading factor λ starts decreasing. Larger step size can be taken if the curve tracing is on the upper part or lower part of PV curve.

The calculated active and reactive powers in affine form \widehat{P}_i , \widehat{Q}_i in (15) and (16) are obtained after substituting \widehat{V}_i , $\widehat{\delta}_i$ from (12) and (13) into (4) and (5) with all AA operations and approximations as follows:

$$\widehat{P}_i = P_i^0 + \sum_{j=1}^{N_P} P_{ij}^P \epsilon_{P_j} + \sum_{k=1}^{N_Q} P_{ik}^Q \epsilon_{Q_k} + \sum_{r=1}^{N_E} P_{ir} \epsilon_r \quad \text{for } i = 1, 2, \dots, N_P \quad (19)$$

$$\widehat{Q}_i = Q_i^0 + \sum_{j=1}^{N_P} Q_{ij}^P \epsilon_{P_j} + \sum_{k=1}^{N_Q} Q_{ik}^Q \epsilon_{Q_k} + \sum_{r=1}^{N_E} Q_{ir} \epsilon_r \quad \text{for } i = 1, 2, \dots, N_Q \quad (20)$$

where \widehat{P}_i , \widehat{Q}_i are active and reactive power injections, respectively, at the i th bus in affine form. P_i^0 , Q_i^0 are central values of active and reactive power injections, respectively, at the i th bus. P_{ij}^P , P_{ik}^Q , P_{ir} are partial deviations of the calculated affine active power injection at the i th bus. Q_{ij}^P , Q_{ik}^Q , Q_{ir} are partial deviations of the calculated affine reactive power injection at the i th bus. ϵ_r are additional noise terms produced due to non-affine operations. N_E is number of new noise variables produced due to non-affine operations, where P_i^0 , Q_i^0 are the midpoints of specified power injection intervals $[P_i^{\min} P_i^{\max}]$ and $[Q_i^{\min} Q_i^{\max}]$, respectively.

After substituting (19) and (20) in (15) and (16), the following compact expression can be derived

$$\mathbf{Ax} = \mathbf{B} + \mathbf{E} \quad (21)$$

where \mathbf{x} are the vector of noises that represent the uncertainties of active and reactive power injections, i.e. $\mathbf{x} = [\epsilon_{P_1} \dots \epsilon_{P_{N_P}} \epsilon_{Q_1} \dots \epsilon_{Q_{N_Q}}]^T$.

The matrices \mathbf{A} , \mathbf{B} and \mathbf{E} are given as

$$\mathbf{A} = \begin{bmatrix} P_{11}^{P'} & \dots & P_{1N_P}^{P'} & P_{11}^{Q'} & \dots & P_{1N_Q}^{Q'} \\ \dots & \dots & \dots & \dots & \dots & \dots \\ P_{N_P 1}^{P'} & \dots & P_{N_P N_P}^{P'} & P_{N_P 1}^{Q'} & \dots & P_{N_P N_Q}^{Q'} \\ Q_{11}^{P'} & \dots & Q_{1N_P}^{P'} & Q_{11}^{Q'} & \dots & Q_{1N_Q}^{Q'} \\ \dots & \dots & \dots & \dots & \dots & \dots \\ Q_{N_Q 1}^{P'} & \dots & Q_{N_Q N_P}^{P'} & Q_{N_Q 1}^{Q'} & \dots & Q_{N_Q N_Q}^{Q'} \end{bmatrix} \quad (22)$$

The matrix \mathbf{A} represents the coefficients of the noise vector \mathbf{x}

$$\mathbf{B} = \begin{bmatrix} P_1^0 - \widehat{P}_{g_1}(1 + \lambda^0 K_{g_1}) + \widehat{P}_{l_1}(1 + \lambda^0 K_{l_1}) \\ \dots \\ P_{N_P}^0 - \widehat{P}_{g_{N_P}}(1 + \lambda^0 K_{g_{N_P}}) + \widehat{P}_{l_{N_P}}(1 + \lambda^0 K_{l_{N_P}}) \\ Q_1^0 - Q_{g_1}^0 + \widehat{Q}_{l_1}(1 + \lambda^0 K_{l_1}) \\ \dots \\ Q_{N_Q}^0 - Q_{g_{N_Q}}^0 + \widehat{Q}_{l_{N_Q}}(1 + \lambda^0 K_{l_{N_Q}}) \end{bmatrix} \quad (23)$$

Matrix \mathbf{B} is an interval column vector

$$\mathbf{E} = \begin{bmatrix} P_{11} & \dots & P_{1N_E} \\ \dots & \dots & \dots \\ P_{N_P 1} & \dots & P_{N_P N_E} \\ Q_{11} & \dots & Q_{1N_E} \\ \dots & \dots & \dots \\ Q_{N_Q 1} & \dots & Q_{N_Q N_E} \end{bmatrix} \begin{bmatrix} \epsilon_1 \\ \dots \\ \epsilon_{N_E} \end{bmatrix} \quad (24)$$

The matrix \mathbf{E} represents the coefficients of extra noise terms generated in each non-affine operations (i.e. sine, cosine and multiplication) multiplied by the column vector of the extra noises. These extra noises ϵ_1 , ϵ_2 , ..., ϵ_{N_E} are replaced with $[-1, 1]$.

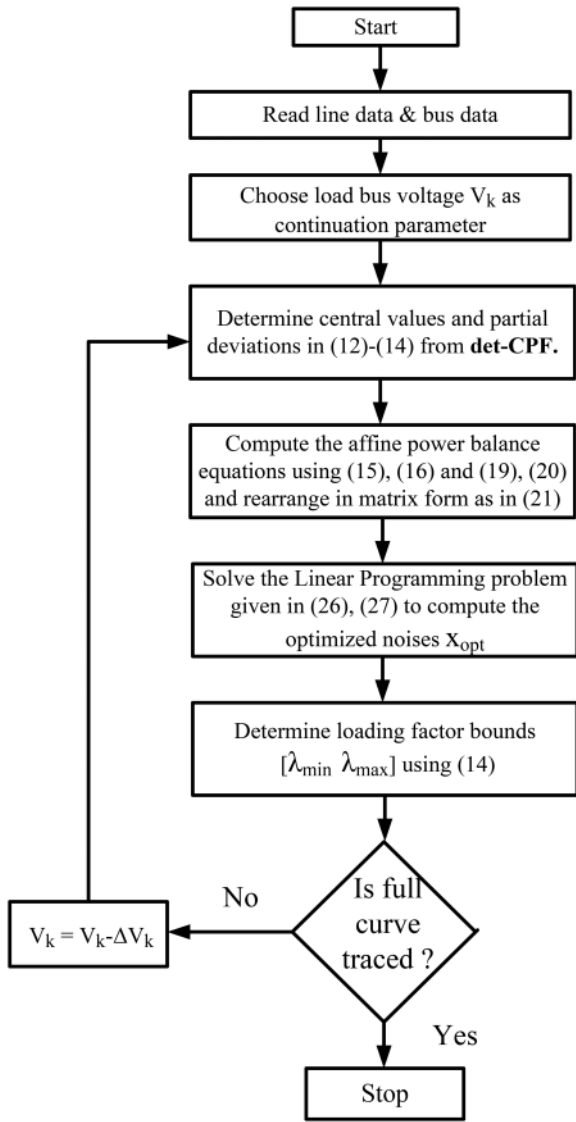


Fig. 1 Flowchart of AA-CPF to compute PV curves

Equation (21) can be further simplified as

$$Ax = C \quad (25)$$

The initial values of all noises in x are $[-1, 1]$. The noise vector x can be contracted so as to satisfy (25). This can be formulated as a dual optimisation problem to obtain the optimised upper and lower bounds of x . This is a simple 'Linear Programming Problem' and is solved as follows.

Equation (26) is solved to find the optimised (minimised) value of upper bounds of x

$$\begin{aligned} \min_{\epsilon_{P_j}, \epsilon_{Q_k}} & \left(\sum_{j=1}^{N_P} \epsilon_{P_j} + \sum_{k=1}^{N_Q} \epsilon_{Q_k} \right) \\ \text{for } & j = 1, \dots, N_P \text{ and } k = 1, \dots, N_Q \\ \text{s.t.} &: -1 \leq \epsilon_{P_j}, \epsilon_{Q_k} \leq 1 \\ \inf(C_i) & \leq \sum_{j=1}^{N_P} A_{ij}\epsilon_{P_j} + \sum_{k=1}^{N_Q} A_{ik}\epsilon_{Q_k} \leq \sup(C_i) \\ \text{for } & i = 1, 2, \dots, N_P + N_Q \end{aligned} \quad (26)$$

Equation (27) is used to get the optimised (maximised) value of lower bounds of x

$$\begin{aligned} \max_{\epsilon_{P_j}, \epsilon_{Q_k}} & \left(\sum_{j=1}^{N_P} \epsilon_{P_j} + \sum_{k=1}^{N_Q} \epsilon_{Q_k} \right) \\ \text{for } & j = 1, \dots, N_P \text{ and } k = 1, \dots, N_Q \\ \text{s.t.} &: -1 \leq \epsilon_{P_j}, \epsilon_{Q_k} \leq 1 \\ \inf(C_i) & \leq \sum_{j=1}^{N_P} A_{ij}\epsilon_{P_j} + \sum_{k=1}^{N_Q} A_{ik}\epsilon_{Q_k} \leq \sup(C_i) \\ \text{for } & i = 1, 2, \dots, N_P + N_Q \end{aligned} \quad (27)$$

The optimised noise vector $x_{\text{opt}} = [x_{\text{min}} \ x_{\text{max}}]$ after solving (26) and (27) is substituted in (14) to get the upper and lower bounds of the loading parameter λ . The load bus voltage at which PV curve to be drawn is decreased step-by-step, and at each step the bounds of λ can be obtained by solving (26) and (27) and PV curve bounds can be plotted. The procedure of AA-CPF is given in the flowchart as shown in Fig. 1.

3.3 Limitations of AA-CPF with existing AA multiplication

Multiplication of AA variables is a non-affine operation which needs an affine approximation. Multiplication is the most commonly used non-affine operation, which needs a better approximation.

The main drawbacks of the existing AA multiplication are:

- Multiplication of any two AA variables results in an additional noise (uncertainty) term. Large systems analyses need to handle many of these extra noise terms due to a large number of multiplication operations. Especially, Chebyshev approximation of sine and cosine functions are the polynomials of the AA variables, where a large number of AA multiplications are needed which leads to even more additional noise terms.
- In the affine approximation given in (11), the last term represents the lumped uncertainty due to all the quadratic terms resulting from the multiplication, i.e. $(\epsilon_1\epsilon_2, \dots, \epsilon_1\epsilon_n, \epsilon_1^2, \dots, \epsilon_n^2)$. The effect of all these quadratic noise terms is being neglected.
- The effect of additional noise term is not included in the objective function in the linear programming problem of the optimisation part. The extra noise term generated in AA multiplication is being neglected as a variable and it is assumed to be $[-1, 1]$ in matrix E from (24) which is not a good approximation and results in overestimation.

4 modAA-based CPF

To overcome the limitations with conventional AA operations especially multiplication, a modAA-based CPF (modAA-CPF) is proposed in the present work which uses the modAA multiplication introduced in [17].

4.1 modAA multiplication

In modAA multiplication [17], a new way of affine approximation of multiplication was introduced which is also conservative and always encloses the true bounds of \hat{w} . In [17], the lumped uncertainty term is distributed proportionally across the existing noise terms to avoid the extra noise term in each multiplication operation and to achieve tighter bounds as given below.

In modAA, multiplication of two generalised AA variables $\hat{u} = (u_0 + \sum_{i=1}^n u_i \epsilon_i)$ and $\hat{v} = (v_0 + \sum_{i=1}^n v_i \epsilon_i)$ is given as follows:

$$\hat{w} = \hat{u} \times \hat{v} = w_0 + \sum_{i=1}^n w_i \left[1 + \frac{w_i}{\sum_{i=1}^n |w_i|} R(\hat{u})R(\hat{v}) \right] \epsilon_i \quad (28)$$

where $w_0 = u_0 \times v_0$ and $w_i = (u_0 \times v_i + v_0 \times u_i)$. The last term of AA multiplication given in (11) is now avoided in (28) of modAA and the quadratic noise terms are proportionally distributed among existing noise terms.

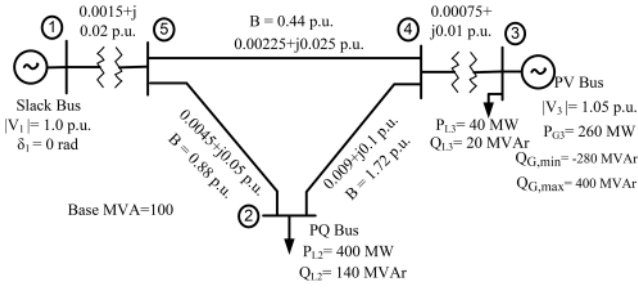


Fig. 2 Single line diagram of 5-bus system

4.2 PV curve computation using modAA-CPF

In modAA-CPF, the affine forms of power balance equations are as follows:

$$\hat{P}_{g_i}(1 + \hat{\lambda}K_{g_i}) - \hat{P}_{l_i}(1 + \hat{\lambda}K_{l_i}) = \hat{P}_i^{\text{modAA}}, \quad i = 1, 2, \dots, N_P \quad (29)$$

$$\hat{Q}_{g_i} - \hat{Q}_{l_i}(1 + \hat{\lambda}K_{l_i}) = \hat{Q}_i^{\text{modAA}}, \quad i = 1, 2, \dots, N_Q \quad (30)$$

Equations (29) and (30) along with parameterisation (17) are solved to obtain PV curve bounds through modAA-CPF.

The affine form bus voltage magnitude and angle is given in (12) and (13) are substituted in (4) and (5) with modAA multiplication given in (28). The calculated active and reactive power affine forms in modAA-CPF \hat{P}_i^{modAA} , \hat{Q}_i^{modAA} are given as follows:

$$\hat{P}_i^{\text{modAA}} = P_i^0 + \sum_{m=1}^{N_P} \mathcal{P}_{im}^P \epsilon_{P_m} + \sum_{n=1}^{N_Q} \mathcal{P}_{in}^Q \epsilon_{Q_n}, \quad \text{for } i = 1, 2, \dots, N_P \quad (31)$$

$$\hat{Q}_i^{\text{modAA}} = Q_i^0 + \sum_{m=1}^{N_P} \mathcal{Q}_{im}^P \epsilon_{P_m} + \sum_{n=1}^{N_Q} \mathcal{Q}_{in}^Q \epsilon_{Q_n}, \quad \text{for } i = 1, 2, \dots, N_Q \quad (32)$$

Substituting (31) and (32) into (29) and (30), the following expression can be derived

$$\mathbf{M}\mathbf{x} = \mathbf{B} \quad (33)$$

where

$$\mathbf{M} = \begin{bmatrix} \mathcal{P}_{11}^{P'} & \dots & \mathcal{P}_{1N_P}^{P'} & \mathcal{P}_{11}^{Q'} & \dots & \mathcal{P}_{1N_Q}^{Q'} \\ \dots & \dots & \dots & \dots & \dots & \dots \\ \mathcal{P}_{N_P 1}^{P'} & \dots & \mathcal{P}_{N_P N_P}^{P'} & \mathcal{P}_{N_P 1}^{Q'} & \dots & \mathcal{P}_{N_P N_Q}^{Q'} \\ \mathcal{Q}_{11}^{P'} & \dots & \mathcal{Q}_{1N_P}^{P'} & \mathcal{Q}_{11}^{Q'} & \dots & \mathcal{Q}_{1N_Q}^{Q'} \\ \dots & \dots & \dots & \dots & \dots & \dots \\ \mathcal{Q}_{N_Q 1}^{P'} & \dots & \mathcal{Q}_{N_Q N_P}^{P'} & \mathcal{Q}_{N_Q 1}^{Q'} & \dots & \mathcal{Q}_{N_Q N_Q}^{Q'} \end{bmatrix} \quad (34)$$

Matrix \mathbf{B} in (33) is the same as in (21). There are no additional noises generated in (31) and (32) due to the incorporation of modAA multiplication. The additional matrix \mathbf{E} as in (21) is eliminated in (33), as all the quadratic noise terms are adjusted in the existing noise coefficients leading to tighter solution bounds.

Similar to AA-CPF described in Section 3, the noise vector \mathbf{x} can be contracted by solving the dual optimisation problem using linear programming as given in (26) and (27) so as to satisfy (33). The initial values of noise vector \mathbf{x} bounds from $[-1, 1]$ are tightened to optimised noise vector $\mathbf{x}_{\text{opt}}^{\text{modAA}} = [\mathbf{x}_{\text{min}}^{\text{modAA}}, \mathbf{x}_{\text{max}}^{\text{modAA}}]$. The optimised noise vector $\mathbf{x}_{\text{opt}}^{\text{modAA}}$ is substituted in (14) to get λ bounds

at each step and PV curves are plotted. The procedure of modAA-CPF to draw PV curve bounds is similar to the flowchart given in Fig. 1.

5 Simulation results

The proposed modAA-CPF considering uncertainty in active and reactive power injections at buses is tested on the 5-bus system [20], IEEE 57 [21], European 1354 [22] and Polish 2383 [22] bus systems. PV curve bounds obtained from the proposed modAA-CPF are compared with those obtained from AA-CPF [16] and MC-CPF [7]. The bounds obtained from MC simulations are the most accurate bounds compared with any other method since it considers a large number of samples of loads and generations to arrive at a solution. Hence, the PV curve bounds obtained from MC-CPF is assumed to be the true solution and is used as a benchmark to compare and to show the validity of the proposed modAA-CPF. An accuracy index (AI) is defined as follows:

$$\text{AI} = \frac{(\text{ML}_{\text{upper}}^{\text{MC}} - \text{ML}_{\text{lower}}^{\text{MC}})}{(\text{ML}_{\text{upper}}^{\text{AA}} - \text{ML}_{\text{lower}}^{\text{AA}})} \times 100 \% \quad (35)$$

where $\text{ML}_{\text{upper}}^{\text{MC}}$, $\text{ML}_{\text{lower}}^{\text{MC}}$ are the upper and lower bounds of maximum loadability in MW obtained from MC-CPF. $\text{ML}_{\text{upper}}^{\text{AA}}$, $\text{ML}_{\text{lower}}^{\text{AA}}$ are the upper and lower bounds of maximum loadability in MW obtained from AA-CPF/modAA-CPF.

5.1 5-Bus test system

The bus and line data for the 5-bus system are given, along with a single line diagram in Fig. 2. The total load of the system is 440 MW. In MC-CPF, 5000 uniformly distributed random samples of active and reactive powers drawn at the load buses and active power generation at the generator buses with ± 10 , ± 20 and $\pm 30\%$ uncertainty are extracted as given below:

$$\begin{aligned} P_{l, \text{sample}} &= P_l^{\text{min}} + (P_l^{\text{max}} - P_l^{\text{min}}) \times \text{rand}(\text{nsample}, 1) \\ Q_{l, \text{sample}} &= Q_l^{\text{min}} + (Q_l^{\text{max}} - Q_l^{\text{min}}) \times \text{rand}(\text{nsample}, 1) \\ P_{g, \text{sample}} &= P_g^{\text{min}} + (P_g^{\text{max}} - P_g^{\text{min}}) \times \text{rand}(\text{nsample}, 1) \end{aligned} \quad (36)$$

where $\text{rand}(\text{nsample}, 1)$ is the column vector of the nsample number of uniformly distributed values within the range of $[0,1]$. $P_{l, \text{sample}}$, $Q_{l, \text{sample}}$, $P_{g, \text{sample}}$ are uniformly distributed samples of load active, reactive and generator active powers of size 'nsample' within the range $[P_l^{\text{min}}, P_l^{\text{max}}]$, $[Q_l^{\text{min}}, Q_l^{\text{max}}]$ and $[P_g^{\text{min}}, P_g^{\text{max}}]$, respectively. det-CPF is applied 5000 times on each sample set of power generation and load and 5000 PV curves are drawn. The lower and upper bounds of PV curves are extracted and are shown in Fig. 3. For computation of PV curves using AA-CPF and modAA-CPF, the constants K_{g_i} , K_{l_i} in (15) and (16) at all buses are assumed to be 1 in the present work.

Fig. 3 shows the PV curve bounds for 5-bus system obtained from MC-CPF, AA-CPF and the proposed modAA-CPF with $\pm 20\%$ uncertainty in active and reactive power injections at all buses. From Fig. 3, it can be observed that the PV curve bounds obtained by the proposed modAA-CPF are closer to the bounds obtained from MC-CPF than that of AA-CPF.

Table 1 shows the maximum loadability/steady-state voltage stability limit intervals using MC-CPF, AA-CPF and the proposed modAA-CPF. In Table 1, it can be observed that the maximum loadability bounds obtained by the proposed modAA-CPF have tighter bounds as compared with AA-CPF. Table 2 gives the AI as given in (35) for both AA-CPF and the proposed modAA-CPF. It can be clearly observed from Table 2 that the proposed method is 8.1, 12.26 and 14.99% more accurate than AA-CPF for an uncertainty range of ± 10 , ± 20 and $\pm 30\%$, respectively.

5.2 IEEE 57-Bus system

The proposed modAA-CPF is implemented on IEEE 57-bus system [21] which supplies a base load of 1250.8 MW. The

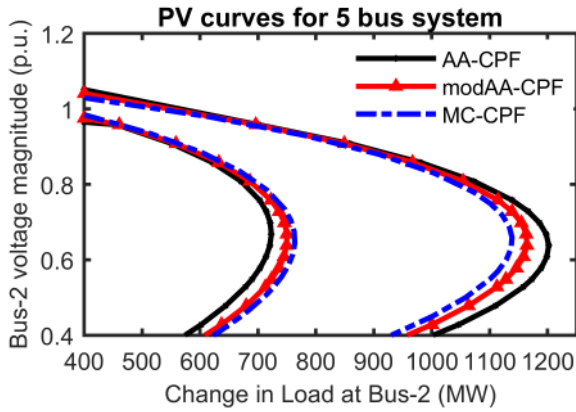


Fig. 3 PV curves for the 5-bus system at bus-2 for $\pm 20\%$ uncertainty

Table 1 Maximum loadability intervals for 5-bus system

Maximum loadability interval [ML _{min} ML _{max}] in MW			
Method	$\pm 10\%$ Uncertainty	$\pm 20\%$ Uncertainty	$\pm 30\%$ Uncertainty
MC-CPF [7]	[830 1013.2]	[763.5 1139]	[703.36 1297.6]
proposed modAA-CPF	[827.6 1016.4]	[749.8 1164]	[689.04 1347.2]
AA-CPF [16]	[820 1026]	[723 1202]	[623.8 1412.8]

Table 2 AI for 5-bus system

Method	$\pm 10\%$ Uncertainty, %	$\pm 20\%$ Uncertainty, %	$\pm 30\%$ Uncertainty, %
AA-CPF [16]	88.93	78.39	75.3
proposed modAA-CPF	97.03	90.65	90.29
improvement in accuracy with the proposed modAA-CPF	8.1	12.26	14.99

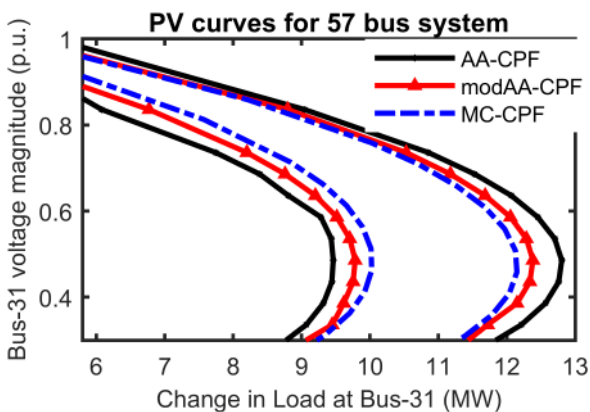


Fig. 4 PV curves for the 57-bus system at bus-31 for $\pm 20\%$ uncertainty

Table 3 Maximum loadability intervals for 57-bus system

Maximum loadability interval [ML _{min} ML _{max}] in MW			
Method	$\pm 10\%$ Uncertainty	$\pm 20\%$ Uncertainty	$\pm 30\%$ Uncertainty
MC-CPF [7]	[10.432 11.617]	[10.03 12.15]	[9.575 12.731]
proposed modAA-CPF	[10.315 11.663]	[9.783 12.37]	[9.0 13.16]
AA-CPF [16]	[10.243 11.781]	[9.463 12.8]	[8.23 14.08]

Table 4 AI for 57-bus system

Method	$\pm 10\%$ Uncertainty, %	$\pm 20\%$ Uncertainty, %	$\pm 30\%$ Uncertainty, %
AA-CPF [16]	77.05	63.53	53.95
proposed modAA-CPF	88.1	81.95	75.92
improvement in accuracy with the proposed modAA-CPF	11.05	18.42	21.97

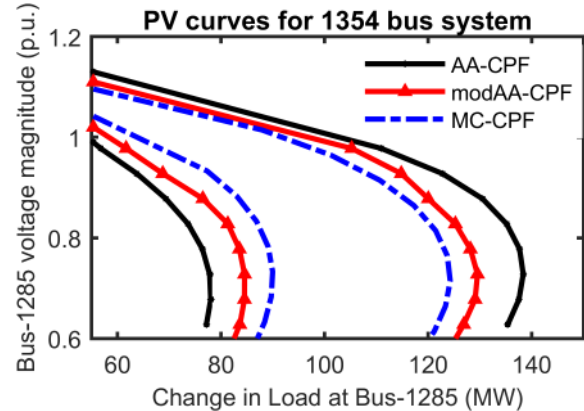


Fig. 5 PV curves for the 1354-bus system at bus-1285 for $\pm 20\%$ uncertainty

Table 5 Maximum loadability intervals for 1354-bus system

Maximum loadability interval [ML _{min} ML _{max}] in MW			
Method	$\pm 10\%$ Uncertainty	$\pm 20\%$ Uncertainty	$\pm 30\%$ Uncertainty
MC-CPF [7]	[98.1 115.25]	[89.97 124.3]	[86.1 128.08]
proposed modAA-CPF	[96.07 117.13]	[84.54 129.5]	[78.35 136.74]
AA-CPF [16]	[94.6 118.72]	[78.01 138.4]	[65.63 149.2]

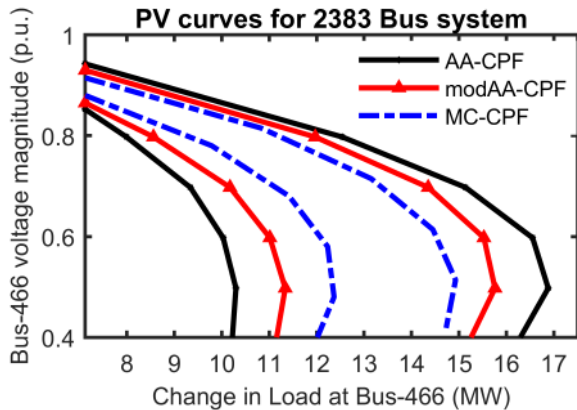
constants K_{g_r} , K_{l_i} in (15) and (16) at all buses are assumed to be 1. The procedure followed for MC-CPF is same as described for 5-bus test case. Fig. 4 shows the PV curve bounds obtained by the proposed modAA-CPF, AA-CPF [16] and MC-CPF [7] for an uncertainty of $\pm 20\%$ in active and reactive power injections at all buses in the system. Table 3 gives the maximum loadability bounds obtained from the proposed modAA-CPF, AA-CPF and MC-CPF. Table 4 shows the AI as given in (35) for the proposed modAA-CPF and AA-CPF. From Tables 3 and 4, it is evident that the proposed method is 11.05, 18.42 and 21.97% more accurate than AA-CPF for an uncertainty range of ± 10 , ± 20 and $\pm 30\%$, respectively.

5.3 1354-Bus test system

The proposed method is tested on 1354 European system [22] which supplies a base load of 73,060 MW. The constants K_{g_r} , K_{l_i} in (15), (16) at all buses are assumed to be 1. The MC-CPF procedure is the same as described in the 5-bus test system. Fig. 5 shows the PV curve bounds of 1354-bus system obtained by the proposed modAA-CPF, AA-CPF [16] and MC-CPF [7] for an uncertainty range of $\pm 20\%$ in active and reactive power injections at all buses in the system. Table 5 gives the maximum loadability bounds obtained from the proposed modAA-CPF, AA-CPF and MC-CPF. Table 6 shows the AI as given in (35) for the proposed modAA-CPF and AA-CPF. From Tables 5 and 6, it is clearly observed that the proposed method is 10.33, 19.5 and 21.66% more accurate than AA-CPF for an uncertainty range of ± 10 , ± 20 and $\pm 30\%$, respectively.

Table 6 AI for 1354-bus system

Method	$\pm 10\%$ Uncertainty, %	$\pm 20\%$ Uncertainty, %	$\pm 30\%$ Uncertainty, %
AA-CPF [16]	71.1	56.85	50.23
proposed modAA- CPF	81.43	76.35	71.896
improvement in accuracy with the proposed modAA- CPF	10.33	19.5	21.66

**Fig. 6** PV curves for the 2383-bus system at bus-466 for $\pm 20\%$ uncertainty**Table 7** Maximum loadability intervals for 2383-bus system for $\pm 20\%$ uncertainty

Method	Maximum loadability interval [ML_{\min} ML_{\max}] in MW		
	Normal operation	Generator 131 trip	Line 138-67 trip
MC-CPF [7]	[12.367 14.931]	[10.962 15.463]	[7.391 10.787]
proposed modAA-CPF	[11.338 15.760]	[8.678 17.252]	[5.35 12.465]
AA-CPF [16]	[10.298 16.88]	[6.499 19.153]	[3.655 14.131]

Table 8 AI for 2383-bus system with $\pm 20\%$ uncertainty

Method	Normal operation, %	Generator 131 trip, %	Line 138-67 trip, %
AA-CPF [16]	38.95	35.57	32.42
proposed modAA-CPF	57.98	52.49	47.73
improvement in accuracy with the proposed modAA-CPF	19.03	16.92	15.31

5.4 2383-Bus system

2383-Bus system [22] represents the portion of the Polish system which supplies a base load of 24,558 MW. Similar to the 5-Bus test system, the constants K_{g_i} , K_{l_i} in (15) and (16) at all buses are taken as 1 for both AA-CPF and modAA-CPF. For MC-CPF, 5000 uniformly distributed random samples of load active and reactive powers and generator active powers at all buses with $\pm 20\%$ uncertainty are extracted as given in (36). The upper and lower bounds of PV curves are extracted from 5000 solutions obtained from det-CPF and plotted as shown in Fig. 6.

Fig. 6 shows the PV curve bounds obtained from the proposed modAA-CPF, AA-CPF and MC-CPF for a 2383-bus system with $\pm 20\%$ uncertainty in active and reactive power injections at all buses. It can be clearly observed from Fig. 6 that the bounds obtained from the proposed modAA-CPF are tighter compared with that of AA-CPF.

The proposed modAA-CPF is also tested for two contingency cases on the 2383-Bus system. The worst contingency is of the line 138-67 tripping, which is the most heavily loaded line in the system and another contingency case is the generator trip which is connected to bus 131. The results are compared with AA-CPF and MC-CPF and are given in Table 7.

Table 7 shows the maximum loadability intervals obtained from the proposed modAA-CPF, AA-CPF and MC-CPF under the normal operating condition, generator 131 and line 138-67 trip conditions for 2383-bus system with $\pm 20\%$ uncertainty. From Table 7, it can be observed that the proposed modAA-CPF gives tighter bounds as compared with AA-CPF. Table 8 gives the AI for AA-CPF and the proposed modAA-CPF for an uncertainty of $\pm 20\%$ and it is observed that the proposed modAA-CPF is 19.03, 16.92 and 15.31% more accurate than AA-CPF under the normal operating condition, generator 131 open and line 138-67 open conditions, respectively. There is a significant improvement in accuracy with the proposed modAA-CPF method under normal conditions and contingency cases as well.

6 Conclusion

A modAA-based CPF analysis is proposed in this paper to compute PV curve bounds under uncertainties associated with active and reactive power injections at buses in the system. The proposed method has an advantage of obtaining tighter PV curve bounds with the use of modAA multiplication which reduces the overestimation of solution bounds caused by the existing AA multiplication. The proposed modAA-CPF is tested on 5-bus test case, IEEE 57, European 1354 and Polish 2383-bus systems. The results obtained by the proposed modAA-CPF method are compared with MC simulations based on MC-CPF and AA-based AA-CPF. From simulation results, it is observed clearly that the proposed modAA-CPF gives tighter PV curve bounds and there is a significant improvement in accuracy as compared with AA-CPF.

7 Acknowledgment

The authors would like to acknowledge the financial support given by Department of Science and Technology, Government of India for the project Indo-UK clean energy research initiative.

8 References

- [1] 'Voltage stability assessment: concepts, practices and tools', IEEE/PES Power System Stability Subcommittee, Technical Report, August 2002
- [2] Ajarapu, V., Christy, C.: 'The continuation power flow: a tool for steady state voltage stability analysis', *IEEE Trans. Power Syst.*, 1992, 7, (1), pp. 416–423
- [3] Chiang, H.-D., Flueck, A.J., Shah, K.S., *et al.*: 'CPFLOW: a practical tool for tracing power system steady-state behavior due to load and generation variations', *IEEE Trans. Power Syst.*, 1995, 10, (2), pp. 623–634
- [4] Neto, A.B., Alves, D.A.: 'Improved geometric parameterisation techniques for continuation power flow', *IET Gener. Transm. Distrib.*, 2010, 4, (12), pp. 1349–1359
- [5] Ju, Y., Wu, W., Zhang, B., *et al.*: 'Continuation power flow based on a novel local geometric parameterisation approach', *IET Gener. Transm. Distrib.*, 2014, 8, (5), pp. 811–818
- [6] Mehta, D., Nguyen, H.D., Turitsyn, K.: 'Numerical polynomial homotopy continuation method to locate all the power flow solutions', *IET Gener. Transm. Distrib.*, 2016, 10, (12), pp. 2972–2980
- [7] da Silva, A.L., Coutinho, I., de Souza, A.Z., *et al.*: 'Voltage collapse risk assessment', *Electr. Power Syst. Res.*, 2000, 54, (3), pp. 221–227
- [8] Rodrigues, A., Prada, R., Da Guia da Silva, M.: 'Voltage stability probabilistic assessment in composite systems: modeling unsolvability and controllability loss', *IEEE Trans. Power Syst.*, 2010, 25, (3), pp. 1575–1588
- [9] Chun-Lien, S., Chan-Nan, L.: 'Two-point estimate method for quantifying transfer capability uncertainty', *IEEE Trans. Power Syst.*, 2005, 20, (2), pp. 573–579
- [10] Zhang, J., Dobson, I., Alvarado, F.L.: 'Quantifying transmission reliability margin', *Int. J. Electr. Power Energy Syst.*, 2004, 26, (9), pp. 697–702
- [11] Greene, S., Dobson, S.G., Alvarado, F.: 'Sensitivity of the loading margin to voltage collapse with respect to arbitrary parameters', *IEEE Trans. Power Syst.*, 1997, 12, (1), pp. 262–272
- [12] Greene, S., Dobson, S.G., Alvarado, F.: 'Sensitivity of transfer capability margins with a fast formula', *IEEE Trans. Power Syst.*, 2002, 17, (1), pp. 34–40
- [13] Senthil Kumar, S., Ajay-D-Vimal, R.P.: 'Fuzzy logic based stability index power system voltage stability enhancement', *Int. J. Comput. Electr. Eng.*, 2010, 2, (1), pp. 24–31

- [14] Vaccaro, A., Canizares, C.A., Villacci, D.: 'An affine arithmetic-based methodology for reliable power flow analysis in the presence of data uncertainty', *IEEE Trans. Power Syst.*, 2010, **25**, (2), pp. 624–632
- [15] Vaccaro, A., Canizares, C.A.: 'An affine arithmetic-based framework for uncertain power flow and optimal power flow studies', *IEEE Trans. Power Syst.*, 2017, **32**, (1), pp. 274–288
- [16] Munoz, J., Canizares, C., Bhattacharya, K., *et al.*: 'An affine arithmetic-based method for voltage stability assessment of power systems with intermittent generation sources', *IEEE Trans. Power Syst.*, 2013, **28**, (4), pp. 4475–4487
- [17] Ma, J.D., Rutenbar, R.A.: 'Fast interval-valued statistical modeling of interconnect and effective capacitance', *IEEE Trans. Comput.-Aided Des. Integr. Circuits Syst.*, 2006, **25**, (4), pp. 710–724
- [18] de Figueiredo, L.H., Stolfi, J.: 'Affine arithmetic: concepts and applications', *Numer. Algorithms*, 2004, **37**, (1), pp. 147–158
- [19] Mason, J., Handscomb, D.: '*Chebyshev polynomials*' (Chapman Hall/CRC, Boca Raton, FL, USA, 2002)
- [20] Duncan-Glover, J., Sarma, S.S., Overbye, T.: '*Power system analysis and design*' (CENGAGE Learning, Independence, KY, USA, 2008)
- [21] Power systems test case archive. Available at <http://www2.ee.washington.edu/research/pstca/>, accessed February 2018
- [22] Zimmerman, R.D., Murillo-Sanchez, C.E., Thomas, R.J.: 'MATPOWER: steady-state operations, planning, and analysis tools for power systems research and education', *IEEE Trans. Power Syst.*, 2011, **26**, (1), pp. 12–19